Electrocatalytic oxidation of ethylene glycol in 0.5 M H_2SO_4 and 0.5 M NaOH solutions at a bimetallic deposited electrode

M[a] Soledad Ureta-Zañartu [a,*], Claudia Yáñez [a], Maritza Páez [b], Gloria Reyes [a]

[a] *Departamento de Ciencias Químicas, Facultad de Química y Biología, Universidad de Santiago de Chile, Casilla 307, Santiago-2, Chile*
[b] *Departamento de Química Aplicada, Facultad de Química y Biología, Universidad de Santiago de Chile, Casilla 307, Santiago-2, Chile*

Received 24 July 1995; in revised form 13 October 1995

Abstract

The activity of Pt, Pt + Pb and Pt + Ir deposits on Ti, for ethylene glycol (EG) oxidation, was studied in both 0.5 M H_2SO_4 and 0.5 M NaOH solutions. The metallic deposits were prepared by electrolysis at constant current on Ti, with their morphology studied by scanning electron microscopy.

These electrodes revealed higher activities in alkaline medium than in acid solutions, the Pt deposits being the most active for EG electro-oxidation. In acid medium, although the electrodes generally showed low electrocatalytic activities, among them Pt + Ir codeposits presented the best performance. Additionally, from activity measurements in acid medium, a synergistic effect for Pt + Ir electrodes was observed. The effect of the supporting electrolyte on the activity of these electrodes is discussed in terms of a reaction path, which is dependent on the OH^- anions in alkaline solutions and on the adsorbed $(OH)_{ad}$ species in sulfuric acid solution.

Keywords: Electrocatalyst; Oxidation; Ethylene glycol; Electrode

1. Introduction

The study of the electrocatalytic reaction on noble metal electrodes with and without modification is a recurrent topic in the scientific literature. These studies refer frequently to two problems: energy storage and fuels cells. The greatest limitation on these processes is of an electrochemical type. Both the anode and the cathode present slow kinetics, hence interest resides in developing electrodes with better catalytic properties [1,2].

The ethylene glycol (EG) molecule is a diol-alcohol that can be obtained from bio-mass and it has the advantages of involving a large number of electrons per molecule in its oxidation, and being a renewable fuel, not toxic and of high reactivity [3,4].

Former studies of ethylene glycol oxidation on noble metal electrodes have demonstrated that these electrodes are electrocatalytic for this reaction [5], especially if the electrodes are modified by underpotential deposition (upd) layers of lead [6,7]. The reactivity of EG is particularly high in alkaline medium on platinum [8]. It is known that electrocatalytic reactions at solid electrodes involve the participation of adsorbed species acting either as reactive intermediates or as a poison, depending on the electrochemical systems. This has generally been associated with variations of the properties of surface oxide films in the electrodes [9]. It is well known that it is possible to modify the specific characteristics of the electrode by incorporating another metal on the bare electrode surface. Examples of modified electroactive surfaces are bimetallic electrodes obtained by upd or deposition of metals in submonolayers. However, these electrodes have the drawback that the other metal (ad-metal) must be dissolved in the electrolyte. Additionally, they have a limited area and reduced stability. Thus, interest in the electrocatalytic behavior of bimetallic electrodes with a large active area per geometric area, which do not require additional metallic ions dissolved in the electrolyte, has been enhanced in view of the wide area of application. In the literature studies with bimetallic electrodes have been reported. For example, Pt + Pd alloys have been used for EG electro-oxidation [10] and Pt + Ir alloys for the electrochemical reduction of H_2O_2 [11]. Considering the catalytic effect of foreign adatoms on the noble metal surface and the relevance for

* Corresponding author.

electrocatalysis of having highly dispersed Pt, we study in this work the electrocatalytic behavior of bimetallic electrodes obtained by electrodeposition of Pt, Pt + Pb and Pt + Ir on Ti electrodes in both 0.5 M H_2SO_4 and 0.5 M NaOH electrolyte. This technique does not need thermal decomposition treatment in the sample preparation. It is known that the surface morphology and microstructure of the deposits are not homogeneous and are greatly influenced by the preparation conditions [12].

2. Experimental

2.1. Electrode preparation

Pt and Pt + M electrodes (with M = Ir or Pb) were prepared by electrolysis at constant current (12 to 15 mA cm^{-2}) of chloroplatinic acid solutions in 0.5 M H_2SO_4 plus the respective salt ($PbCO_3$ or $Na_2IrCl_6 \cdot 3H_2O$) on Ti. Titanium foils (99.7%) having dimensions $10 \times 10 \times 0.25$ mm^3 were washed previously in concentrated sulfuric acid and then treated in the usual way [13] by cyclic voltammetry (CV) for 2 h in 0.5 M H_2SO_4 between −0.23 and 1.10 V (SCE). The electrodes thus prepared revealed deposits of good adherence and no ohmic components in the CV curves.

2.2. Electrode characterization

The electrodes were characterized in 0.5 M H_2SO_4 by cyclic voltammetry. In the case of Pt + Pb deposits, to avoid a massive dissolution of lead, the potential was scanned from the H_2 evolution potential ($E_c = -0.23$ V in 0.5 M H_2SO_4) to 1.15 V more positive than the initial potential E_c [14].

A conventional three-compartment Pyrex cell, provided with a Luggin capillary, was employed. All potentials were measured with respect to, and are referred in the text to, a saturated calomel electrode (SCE). A Pt spiral of ca. 8 cm^2 was used as a counter electrode, which was separated from the main compartment by a wet conical stopcock. Electrical contact was achieved through the thin liquid electrolyte film wetting the cone. The complete set up has been described elsewhere [15,16]. Voltammetric measurements were performed at 20°C under nitrogen. The real electrode areas were estimated from CV curves in 0.5 M H_2SO_4 solutions. The procedure described before [17,18] involves integration of the charge due to hydrogen adsorption (desorption) and oxygen adsorption. For Pt-electrodeposited electrodes a charge value of 224 $\mu C\ cm^{-2}$ was used [19] to represent full hydrogen coverage for 1 cm^2 of active surface area of Pt. For this electrode the charge involving oxygenated species, in the potential window used, was estimated at 350 $\mu C\ cm^{-2}$ (active area). The latter was used to estimate the active area of Pt + Pb and Pt + Ir electrodes. Oxidation of EG was investigated using CV in both 0.5 M H_2SO_4 and 0.5 M NaOH solutions.

The surface morphology was studied by scanning electron microscopy (SEM) with a Siemens Autoscan apparatus. To determine the proportion of both metals in the Pt + M codeposit, flame spectrophotometry was employed. To carry out the analysis, the electrodes were dissolved previously in concentrated HCl. For Pt a spectrophotometer, Perkin-Elmer model 4000, was used with a lamp of hollow Pt cathode at 265.9 nm. For Pb, GBC 905 equipment was used with a lamp of hollow Pb cathode at 217 nm.

3. Results and discussion

3.1. Pt electrodes

In order to select the electrolyte used in the electrode preparation, the morphology and electrocatalytic activity of Pt deposits formed in 0.5 M H_2SO_4 and 1 M HCl was investigated. SEM images, showing the surface morphology, are presented in Fig. 1. The aspect of the surface in Fig. 1 shows light spots associated with the presence of Pt deposits on the macroscopic surface. The dark regions seem to be related to the absence of deposits and/or with a surface region where microscopic particles of Pt deposits were formed. A comparison of these images reveals a greater size of particles in the Pt deposit and a more homogeneous deposit for the electrodes formed in H_2SO_4. However, in spite of the different deposit morphologies, the voltammetric responses on both electrodes in 0.5 M H_2SO_4 were similar. Additionally, the voltammetric response in the presence of EG was independent of the preparation of the deposits.

From previous results [13], both electrodes may be suitable for use as an anode for ethylene glycol oxidation. Nevertheless, to avoid the presence of Cl^- ions in the deposit, the medium selected for preparation of the electrodes was sulfuric acid. Experimental measurements made previously in this laboratory [13] involving formic acid oxidation on these electrodes indicated that an increase in the electrolysis time only gives rise to an increase in the grain size of the deposit without affecting the electrocatalytical activity of these electrodes. On the basis of these results, in the present work we have used short deposition times and, therefore, thin films of Pt on Ti.

Fig. 2(A) shows the voltammograms of Pt deposits in 0.5 M H_2SO_4 with (solid line) and without (dashed line) 0.1 M EG. Without the organic compound, the *I/E* profile is similar to the voltammograms for platinized platinum electrodes reported in the literature [20]. In the presence of EG, the voltammogram exhibits a wide anodic peak in both scans, positive and reverse. In the positive scan, a shoulder (IIa) before the peak (Ia) and a decrease of the electric charge associated with hydrogen desorption are

observed. The latter indicates that adsorption of some organic residue occurs on the electrode surface, blocking the sites for hydrogen adsorption. In the back scan an anodic current peak (IIIac), which appears at a potential lower than the peak Ia, is revealed.

Studies of the stability of the electrode and its electrocatalytic activity in acid media were carried out by evaluating the charges associated with the hydrogen processes (Q_H) and the formation of oxygen containing species (Q_O) after repetitive cyclic voltammetry (RCV). The variation of these charges with cycling time, under stirring conditions and in the absence and presence of EG (Q_{eg}), is presented in Fig. 2(B). It seems clear from Fig. 2(B) that Q_H decreases significantly in the first CV curve, but Q_O and Q_{eg} seem to decrease more slowly and, consequently, an increase of the real activity probably occurs during continous cycling.

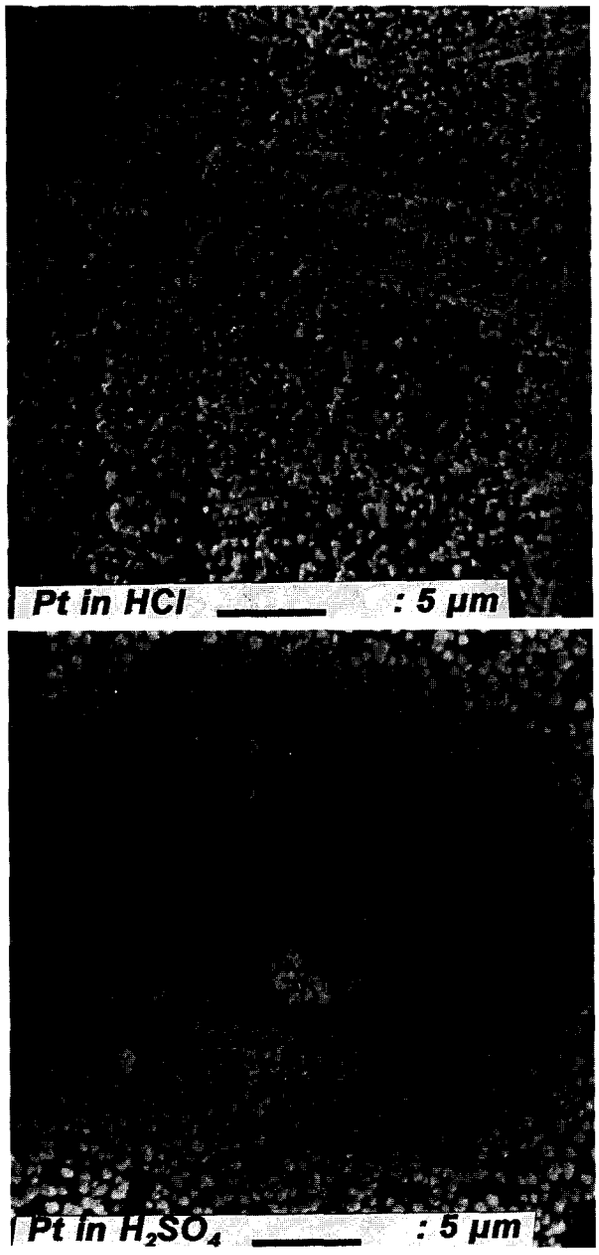

Fig. 1. SEM images of Pt deposits on Ti formed by electrolysis of chloroplatinic acid solution in 1 M HCl and 0.5 M H_2SO_4.

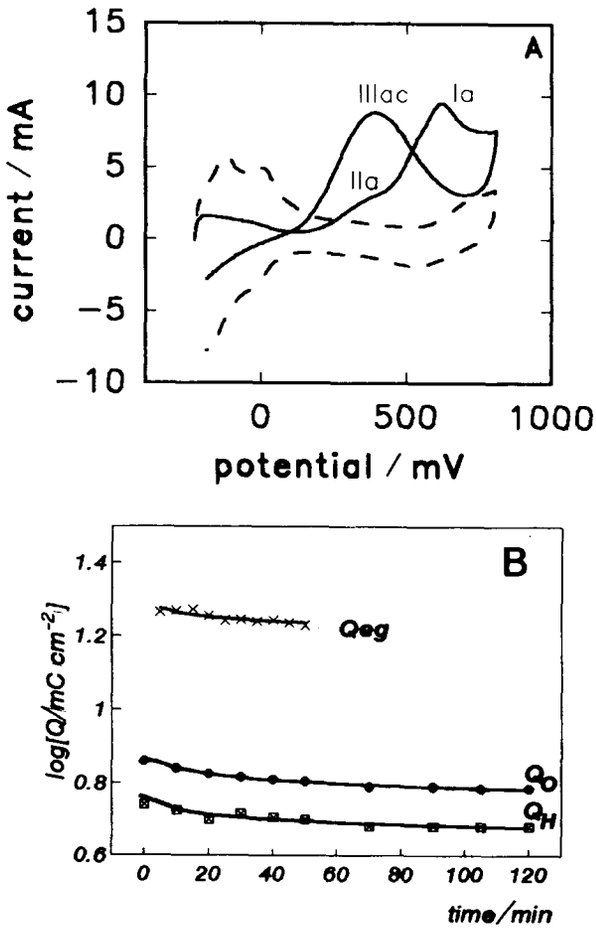

Fig. 2. (A) Cyclic voltammograms obtained on a Pt deposit in 0.5 M H_2SO_4 at 0.1 V s^{-1} with (solid line) and without (dashed line) 0.1 M EG. (B) Variation of Q_O and Q_H on Pt deposits with cycling time at 0.1 V s^{-1} in the absence of EG and of Q_{eg} in the presence of EG.

In alkali, the oxidation of EG proceeds to a greater extent than in acid medium. The CV resembles more a polarization curve than a voltammogram (see Fig. 3). Since measurements on Ti foils, in acid and alkaline medium, did not reveal any activity for the EG oxidation, differences in activity of the codeposits in alkaline medium can apparently be associated with a cooperative effect of the Ti surface. It is well known that Ti forms oxide + hydroxide layers in alkali [21,22], which may promote a bifunctional character of the Pt deposits. Ti foil did not present any activity for the electro-oxidation of EG in either acidic or alkaline medium. Consequently, activity measurements were made with electrodes obtained on different supports and compared with those made with a Pt foil electrode (see Figs. 4(A) to 4(C)). The results do not indicate any effect of the support on the electrocatalytic activity.

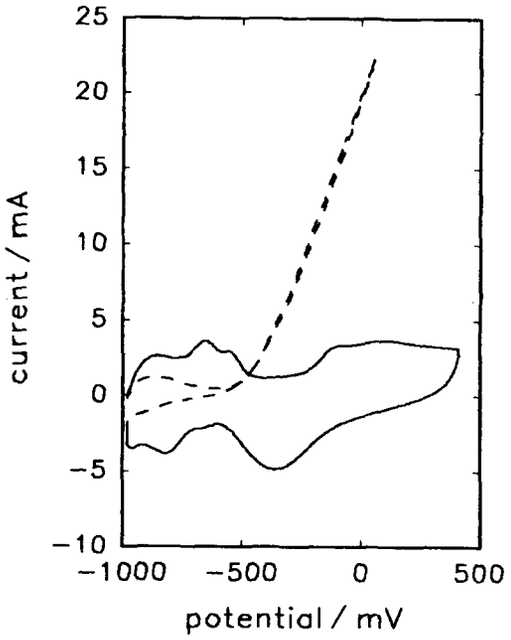

Fig. 3. Cyclic voltammograms obtained on a Pt deposit in 0.5 M NaOH at 0.1 V s^{-1} with (dashed line) and without (solid line) 0.1 M EG.

3.2. Pt + Pb electrodes

Pt + Pb electrodes were obtained under the same experimental conditions as the Pt electrodes, but with the electrolyte saturated with $PbSO_4$. Owing to the low solubility of $PbSO_4$, formed when the $PbCO_3$ salt is dissolved in 0.5 M H_2SO_4, in our studies of the influence of lead concentration in the electrode 1 M HCl was used as supporting electrolyte. In this way it was possible to vary the lead content in the electrolyte and, hence, in the deposit.

Fig. 5 shows the Pt + Pb codeposits on Ti before and after cycling for 2 h in 0.5 M H_2SO_4. In Fig. 5(A), the "cauliflower" like appearance of the deposits is evident. However, as a result of cycling in sulfuric acid, there is a change in appearance (Fig. 5(B)), revealing a decrease in deposit particle size and differently contrasted regions over

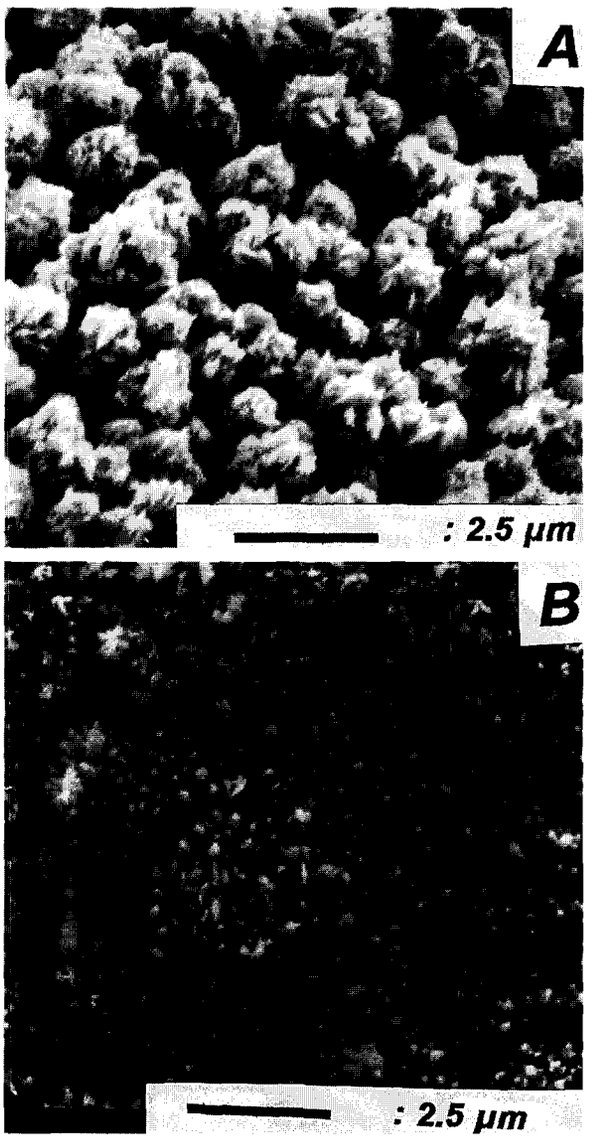

Fig. 5. SEM images showing the morphology of Pt+Pb codeposits before (A) and after (B) cycling the electrode in 0.5 M H_2SO_4 at 0.1 V s^{-1} for 2 h.

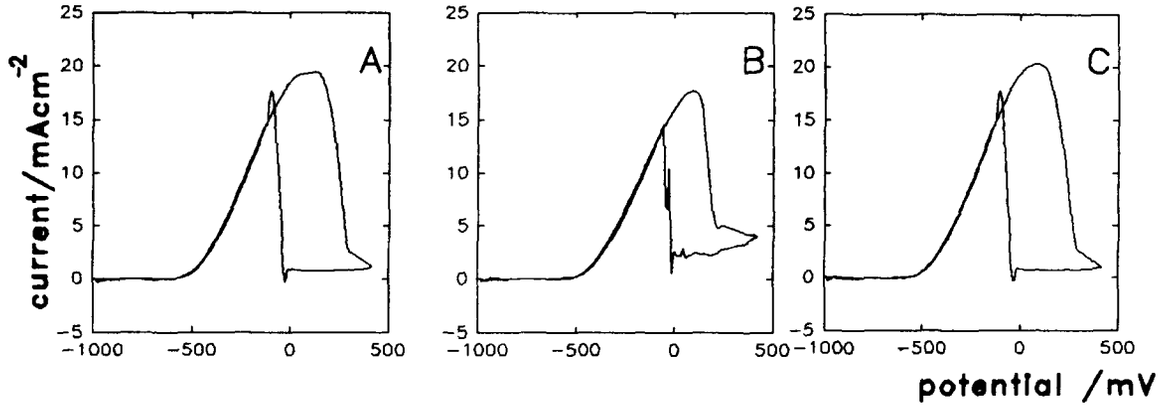

Fig. 4. Cyclic voltammograms obtained on different Pt electrodes in 0.5 M NaOH at 0.002 V s^{-1}. The electrodes are: (A) Pt deposited on Pt, (B) Pt deposited on Ti and (C) Pt foil.

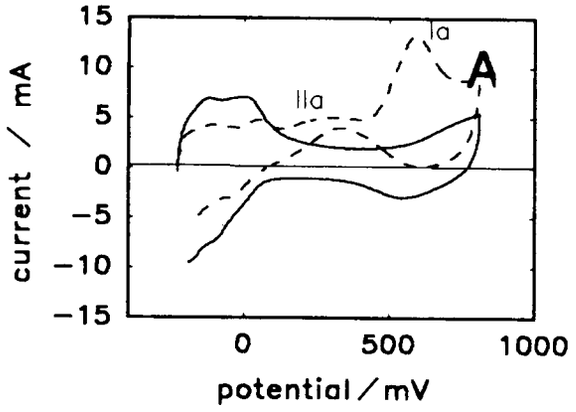

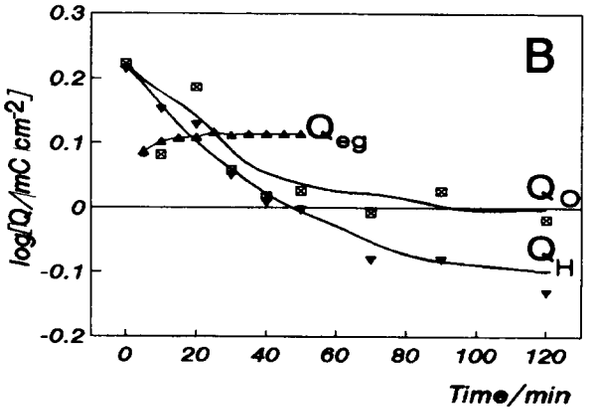

Fig. 6. (A) Cyclic voltammograms obtained on a Pt + Pb codeposit in 0.5 M H_2SO_4 at 0.1 V s^{-1} with (dashed line) and without (solid line) 0.1 M EG. (B) Variation of Q_O and Q_H on Pt deposits with cycling time at 0.1 V s^{-1} in the absence of EG and of Q_{eg} in the presence of EG.

the electrode surface. Similar results have been reported earlier by the authors in a study of formic acid oxidation on bimetallic electrodes [13].

Owing to the high solubility of the PbO oxide in alkaline medium, the study of Pt + Pb deposits on Ti was only carried out in acid medium.

The potentiodynamic profile of the Pt + Pb codeposits in 0.5 M H_2SO_4 is shown in Fig. 6(A) both without (solid line) and with (dashed line) EG in the electrolyte. In the absence of EG, the I/E curves are similar to those of the Pt deposit in H_2SO_4 solutions. In the presence of the organic compound, an oxidation peak current in both directions of the scan is observed. However, in comparison with Pt deposits (Fig. 2(A)), the current peak in the reverse scan is lower, probably as a consequence of a very low coverage in lead. This will be discussed later in this work.

The stability of the electrode in acid medium was studied by evaluating the charges, in the positive scan with and without EG in the electrolyte, after cycling the electrode for different times. The corresponding charges were

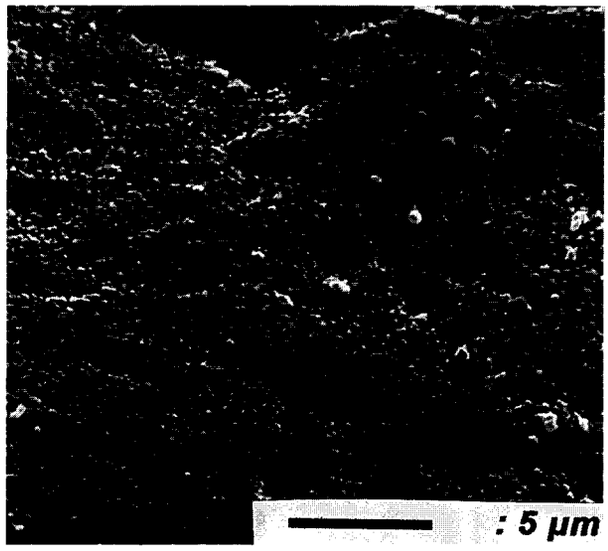

Fig. 7. SEM image of Pt + Ir codeposits on Ti foil.

Q_{eg} (associated with EG electro-oxidation) and Q_O and Q_H (associated with oxide formation and hydrogen desorption in the absence of organics). A plot of the respective charge values vs. the cycling time (Fig. 6(B)) reveals a decrease in the charge values related to hydrogen and oxide species. This may be the result of partial dissolution or sintering processes of Pt + Pb electrodes, which seems to be related to the low catalytic activity of these elec-

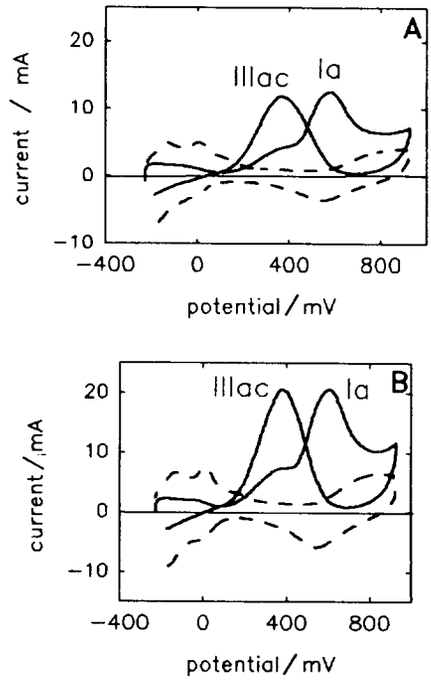

Fig. 8. Cyclic voltammograms obtained on Pt + Ir codeposits in 0.5 M H_2SO_4 at 0.1 V s^{-1} with (dashed line) and without (solid line) 0.1 M EG. (A) Pt:Ir 30:70 and (B) Pt:Ir 70:30.

trodes for EG oxidation (Fig. 6(A)). Variations of the Pt + Pb ratio in the electrolyte revealed changes in Pt:Pb deposit composition and catalytic activity of these electrodes. This will be discussed later in this work.

3.3. Pt + Ir electrodes

These electrodes were obtained in sulfuric acid electrolyte containing different proportions of Ir and Pt salts. The results indicate that the Ir:Pt proportions obtained in the deposits are similar to those in the forming electrolyte. SEM images showing the surface morphology of this electrode (Fig. 7) reveal differently contrasted areas associated with Pt + Ir deposits. In comparison with Pt deposits (Fig. 1), Ir + Pt deposits present a more uniform distribution. This seems to be related to clustering processes of the Ir + Pt deposit particles during electrode preparation. In relation to Ir + Pt deposits, the presence of separate phases for Pt and Ir is considered unlikely, although the phase diagram for Pt + Ir at room temperature presents a region of total immiscibility [23]. The conventional current–potential response for Pt:Ir electrodes, 70:30 and 30:70 in the absence and presence of EG, is shown in Fig. 8. The I/E profile obtained without EG (dashed line) presents the characteristic areas described for a Pt electrode. However, in the presence of EG (solid line) the I/E curves vary, depending on the Pt:Ir proportion (Figs. 8(A) and 8(B)) and the scan rate used. In Fig. 9 the values of I_p and E_p are represented for the three main peaks of Figs. 8(A) and 8(B) as a function of scan rate. The slope values of the different straight lines are summarized in Table 1.

Comparing the results for the two Pt + Ir deposits (Table 1), $\partial \log I_p/\partial \log v$ values of the three current peaks are relatively similar, however, differences are evident for the $\partial E_p/\partial \log v$ values. The greatest differences appear in the peak Ia that corresponds to the oxidation of EG via a strongly adsorbed intermediate and may be attributed to the differences in iridium content of these electrodes. From Figs. 9(C) and 9(D), the EG oxidation on Pt:Ir 30:70 starts at a potential less positive than on Pt:Ir 70:30 (peak Ia). Relating the previous information to voltammetric studies on an Ir electrode under similar experimental conditions [16], the starting potential for the EG oxidation in Pt:Ir 30:70 coincides with the potential of formation of the oxygenated species on the Ir electrode. Thus it is apparent that, while the Pt:Ir 70:30 electrode behaves similarly to the Pt deposit electrodes, the Pt:Ir 30:70 electrode behaves like the Ir electrodes. The latter is additionally confirmed by comparison of the $\partial E_p/\partial \log v$ values for the two Pt + Ir electrodes. These values differ substantially, suggesting a

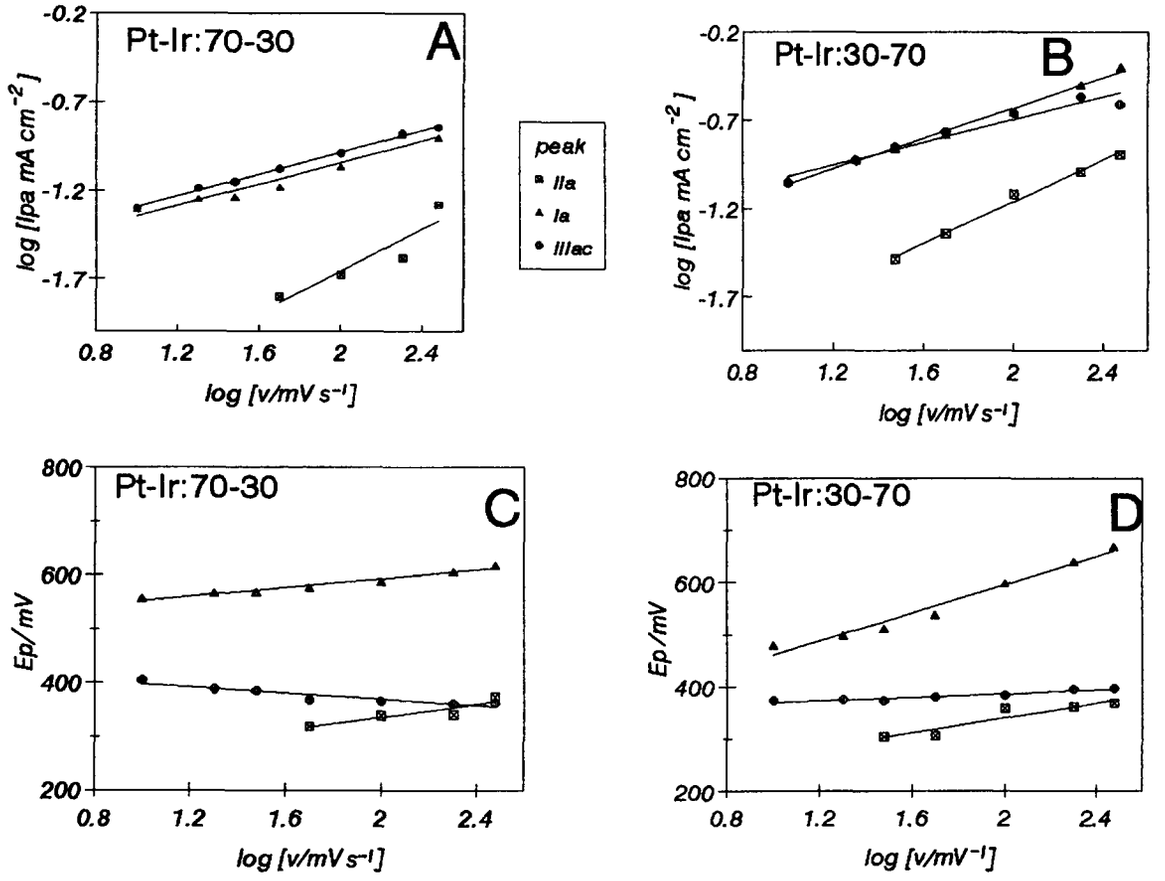

Fig. 9. Variations of $\log I_p$ (A and B) and E_p (C and D) with $\log v$ for EG oxidation on two Pt + Ir electrodes.

Table 1
Summary of the slope in Fig. 9

Composition	Pt:Ir 70:30	Pt:Ir 30:70
$\partial \log I_p / \partial \log v$		
I	0.307	0.432
II	0.597	0.591
III	0.312	0.323
$(\partial E_p / \partial \log v)$/mV dec^{-1}		
I	40.57	134
II	59	70
III	−28.46	17.8

different reaction path on the two electrodes. The difference, which must be related to the stabilization of the intermediate in the electrode surface, is considered, as suggested previously, to be associated with the chemical nature of the metal deposit (Pt or Ir) making up the greater part of these electrodes. The value determined for the $\partial \log I_p / \partial \log v$ slope is less than 0.5; hence, in spite of the complex conditions of this system, it is possible to suppose that there is a control of the reaction different from diffusion or adsorption control.

In alkali, the behavior of the Pt + Ir electrode also resembles a polarization curve with high current. In Fig. 10(A) a cyclic voltammogram obtained at a voltage scan of 100 mV s^{-1} is presented, and in Fig. 10(B) a polarization curve recorded at a voltage scan of 1 mV s^{-1}. In the cyclic voltammogram a marked decrease of the hydrogen charges and an important current intensity in the potential region of the EG oxidation are observed. However, from the polarization curve (Fig. 10(B)) it is not possible to identify a Tafel region. This may indicate that the mechanism of the reaction is complex where the rate determining reaction has to be a function of the potential. Furthermore, from Fig. 10(B) the current density (on the active area of the electrode) measured at the same potential is greater for the electrode with lower iridium content.

4. General discussion

The results obtained for EG oxidation in acid medium indicate a low catalytic activity for the three electrodes. However, differences in the activity of these electrodes can be observed. This is shown in a more explicit way in Fig. 11, which plots I/I° vs. E where I and I° correspond to the current obtained at 5 mV s^{-1} in the absence and presence of EG respectively. From Fig. 11 the activity of the Pt + Ir electrode is 1.5 times greater than that of the Pt or Pt + Pb electrodes. However, in the Pt + Pb electrodes with greater Pb content, the reaction starts at a much less positive potential, which suggests that in this electrode the intermediate is less stabilized and hence is easier to oxidize.

The mechanism of the electro-oxidation of EG is far from being understood. Orts et al. [24], working with Pt monocrystals, have suggested that the reaction mechanism of EG oxidation is similar to that of methanol oxidation on Pt. This means that there would be a mechanism similar to those proposed by Parsons and coworkers [25,26] for HCOOH oxidation on Pt and used by Herrero et al. [27] for HCOOH oxidation on Pt(100) electrodes. There is agreement in these mechanisms in the cleaving of the C–C bond to give products with only one carbon. In this way, the most probable mechanism is that the EG oxidation occurs via a poison intermediate through dehydrogenation in several consecutive steps, forming a species of the type M_xCOH where M represents a surface site on the electrode and x represents the number of surface sites blocked by the adsorbed species. For Pt–HCOOH, this number appears to be dependent on the experimental conditions [28,29] and values between 1 and 3 have been reported. The rate-determining step of the reaction would correspond to the desorption of the M_xCOH species to give CO_2, which can occur (for $x = 3$) according to the following reaction:

$$M_3COH + 3(M\text{–}OH) \longrightarrow CO_2 + 6M + 2H_2O \quad (1)$$

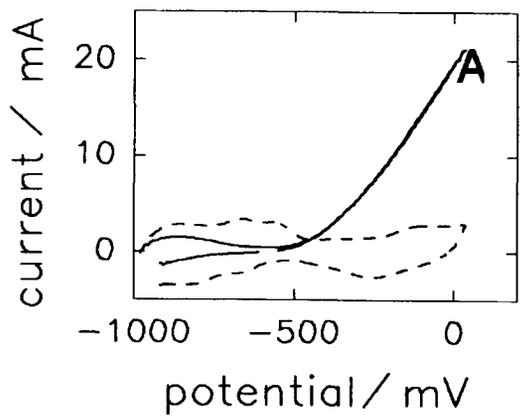

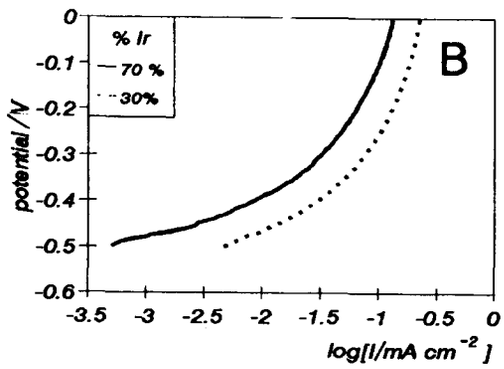

Fig. 10. (A) CV curves on Pt + Ir electrodes at 0.1 V s^{-1} in 0.5 M NaOH with and without EG. (B) Polarization curves obtained at 1 mV s^{-1} on the same electrode.

The interaction of the species M–OH with the adsorbed intermediate M_3COH will depend on the affinity of the adsorbed species with both the codeposit metals and the bare metal region (if it exists). The electrochemical behavior of these electrodes is difficult to interpret from the inter-relationship between acid-base and redox properties. The codeposited metal can promote the formation of unstable M–OH, which facilitates EG oxidation. The reaction (1) can be catalyzed by increasing the M–OH coverage. Studies carried out in our laboratory, encompassing Ir electrodes modified with adatoms for the methanol oxidation, showed that the presence of metallic adatoms modifies the kinetics of such a reaction [15]. From our results, Pt + Ir electrodes have the greater electrocatalytic activity for EG oxidation in acid medium. This is possibly related to the iridium electrode behavior in acid medium, where the formation of oxygenated compounds through the oxy-hydroxy-hydrated species starts at a potential less positive than that for the Pt electrode. These species acting as donors of OH species may increase the reaction rate. In the case of the electrode with lead this was not observed, which is probably due to the greater affinity of lead for OH species, increasing the Pb dissolution rate by oxide formation.

The oxidation of EG in alkaline solution on Pt gives oxalate as the reaction product and can be represented as

$$C_2H_4(OH)_2 + 10OH^- \longrightarrow C_2O_4^{2-} + 8H_2O + 8e^- \quad (2)$$

It has also been suggested that the EG oxidation in alkaline medium involves the adsorption of EG and the dehydrogenation of adsorbed species, as follows:

$$C_2H_4(OH)_2 + Pt + OH^- \rightleftharpoons (residue)_{ad} + H_2O + e^- \quad (3)$$

where a wide variety of reaction intermediates and products has been reported [30].

The role of the $(OH)_{ad}$ species in the mechanism of EG oxidation needs further elucidation [3]. From our results, currents were obtained on Pt deposits in alkaline medium which were even higher than those on Pt + Ir codeposits in acid medium. To elucidate the possible role of the support metal (Ti) in the activity of these electrodes in alkaline medium, additional experiments including Pt deposits on different support metals were carried out (Fig. 4). From the current values, measured at the same potential, the activity of these electrodes is shown to be independent of the support metal. Consequently, the high electrocatalytic properties of the Pt deposits on Ti for EG oxidation in alkaline medium seem to be associated with the role of the OH^- species in solution.

The most probable rate-determining step on Pt and Pt + Ir deposits is the reaction of adsorbed dehydrogenated EG with OH species. However, regarding the differences observed in both electrolytes, it is possible that such OH species are present in alkaline medium (the OH^- ions in the solution $(OH^-)_{aq}$), while in sulfuric acid solution the OH is adsorbed on the electrode $(OH)_{ad}$.

The activity of the Pt + Pb electrodes for EG oxidation was unexpected, since for such a reaction electrodes prepared by upd of Pb in Pt present high activities. Although flame spectroscopic analysis of Pt + Pb deposits revealed Pt:Pb proportions similar to those in the electrolyte, the analysis only gave the total Pt and Pb in the deposits and not the Pt and Pb surface contents. Thus, it is possible that the lower activity of the Pt + Pb deposits is related to a decrease of the Pb sites for EG oxidation. Furthermore, comparing the activity of Pt + Pb deposits with those of Pb on Pt formed by upd, another important aspect to be considered is the behavior of Pb during CV. In an under-

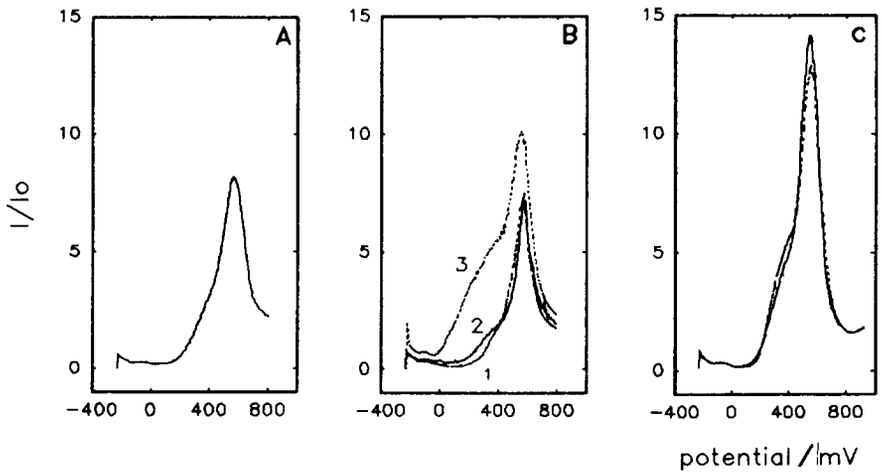

Fig. 11. Plot of the ratio I/I° vs. E, $v = 0.1$ V s^{-1}, with I and I° representing the electro-oxidation current in 0.5 M H_2SO_4 in the presence and absence of 0.1 M EG. (A) Pt electrode, (B) Pt + Pb electrode with different lead content (increase Pb as 1 → 3) and (C) Pt + Ir with two proportions of Pt and Ir.

potential deposit, the Pb coverage is regenerated in each voltammetric cycle. However, in the massive deposit, lead atoms possibly do not behave in a reversible way, therefore decreasing the population of the active sites.

The results obtained indicate the relevance of having species that promote the OH adsorption which occurs with the Pt + Ir electrode. It is important also to emphasise that the preparation method of a codeposited electrode of great active area is simple and very reproducible.

Acknowledgements

The authors are grateful to DICYT-USACH for its support through grant 90-32-uz and to FONDECYT for grant 193093.

References

[1] C. Lamy, Electrochim. Acta, 29 (1984) 1581.
[2] G.R. Mundy, R.J. Porter, P.A. Christensen and A. Hamnett, J. Electroanal. Chem., 279 (1990) 257.
[3] F. Kadirgan, B. Beden and C. Lamy, J. Electroanal. Chem., 136 (1982) 119.
[4] F. Kadirgan, B. Beden and C. Lamy, J. Electroanal. Chem., 143 (1983) 135.
[5] S. Ureta-Zañartu, M.E. Pinto and J. Zagal, Bol. Soc. Chil. Quim., 33 (1988) 83.
[6] M.S. Ureta-Zañartu and C. Ureta-Zañartu, Ann. Quim., 86 (1990) 321.
[7] N. Dalbay and F. Kadirgan, Electrochim. Acta, 36 (1991) 353.
[8] E. Santos and M.C. Giordano, J. Electroanal. Chem., 30 (1985) 871.
[9] M.S. Ureta-Zañartu and C. Yáñez, submitted to J. Electroanal. Chem.
[10] S. Wasmus and W. Vielstich, J. Appl. Electrochem., 23 (1993) 120.
[11] E. Pastor, S. Wasmus, T. Iwasita, M.C. Arévalo, S. González and A.J. Arvía, J. Electroanal. Chem., 350 (1993) 97.
[12] K. Kameyama, K. Tsukada, K. Yahikozawa and Y. Kakasu, J. Electrochem. Soc., 141 (1994) 643.
[13] M.S. Ureta-Zañartu, P. Bravo, F.J. Gil-Llambías, M. Páez and J. Zagal, Bol. Soc. Chil. Quím., 40 (1995) 41.
[14] I. Bakos and G. Horanyi, J. Electroanal. Chem., 332 (1992) 47.
[15] M.S. Ureta-Zañartu, P. Bravo and J.H. Zagal, J. Electroanal. Chem., 337 (1992) 241.
[16] J.H. Zagal, R.M. Vera and M.S. Ureta-Zañartu, J. Electroanal. Chem., 291 (1990) 123.
[17] B. Beden, F. Hahn, J.M. Leger, C. Lamy, C.L. Perdriel, N.R. de Tacconi, R.O. Lezna and A.J. Arvía, J. Electroanal. Chem., 301 (1991) 129.
[18] S. Trasatti and O.A. Petrii, J. Electroanal. Chem., 327 (1992) 353.
[19] J.O'M. Bockris and K.T. Jeng, J. Electroanal. Chem., 330 (1992) 541.
[20] K. Franaszczuk and J. Sobkowski, J. Electroanal. Chem., 261 (1989) 223.
[21] A. Giatti and L.K. Koopal, J. Electroanal. Chem., 352 (1993) 107.
[22] Yu.E. Roginskaya, O.V. Morozova, G.I. Kaplan, R.F. Shifrina, M. Smirnov and S. Trasatti, Electrochim. Acta, 38 (1993) 2435.
[23] ASM Handbook, Alloy Phase Diagrams, Vol. 3, ASM International, The Materials Information Society, New York, 1992, p. 266.
[24] J.M. Orts, A. Fernández Vega, J.M. Feliú, A. Aldaz and J. Clavilier, J. Electroanal. Chem., 290 (1990) 119.
[25] A. Capon and R. Parsons, J. Electroanal. Chem., 44 (1973) 239.
[26] R. Parsons and T. VanderNoot, J. Electroanal. Chem., 257 (1988) 9.
[27] E. Herrero, J.M. Feliú and A. Aldaz, J. Electroanal. Chem., 368 (1994) 101.
[28] T. Iwasita and W. Vielstich, J. Electroanal. Chem., 250 (1988) 452.
[29] W. Vielstich, P. Christensen, S.A. Weeks and A. Hamnett, J. Electroanal. Chem., 242 (1988) 327.
[30] N.M. Markovic, M.L. Avramov-Ivic, N.S. Marinkovic and R.R. Adzic, J. Electroanal. Chem., 312 (1991) 115.